Flavor decomposition for the proton unpolarized, helicity and transversity parton distribution functions

[arXiv:2106.16065]

Floriano Manigrasso

University of Cyprus   University of Rome "Tor Vergata"
Humboldt University of Berlin

In collaboration with:
Constantia Alexandrou, Martha Constantinou,
Kyriakos Hadjiyiannakou, Karl Jansen

The 38th International Symposium on Lattice Field Theory
July 26-30, 2021

LATTICE21
JULY 26-30 2021, ZOOM/GATHER@MIT

STIMULATE
European Joint Doctorates

Overview

Motivation:

- Parton distribution functions play a key role in the on-going experimental program of major facilities BNL, CERN, DESY, Fermilab, JLab and SLAC;
- Accessed experimentally in deep-inelastic scattering (DIS), semi-inclusive DIS, Drell-Yan, and proton-proton scattering processes;
- Strange PDFs resulting from phenomenological analysis show large uncertainties;

Overview

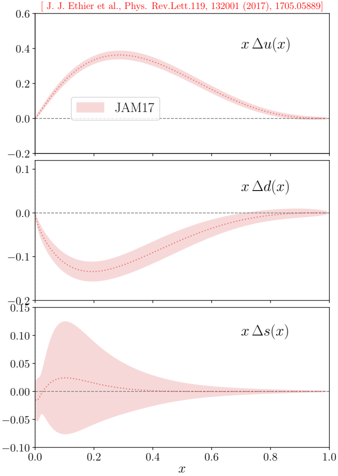

Motivation:

- Parton distribution functions play a key role in the on-going experimental program of major facilities BNL, CERN, DESY, Fermilab, JLab and SLAC;
- Accessed experimentally in deep-inelastic scattering (DIS), semi-inclusive DIS, Drell-Yan, and proton-proton scattering processes;
- Strange PDFs resulting from phenomenological analysis show large uncertainties;

Overview

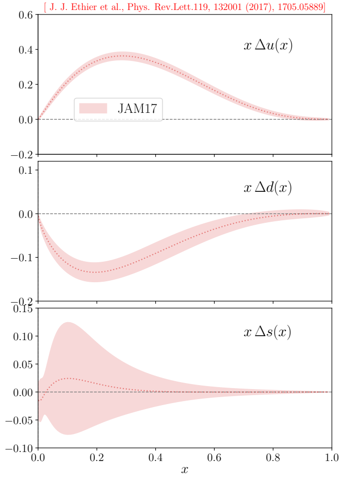

Motivation:

- Parton distribution functions play a key role in the on-going experimental program of major facilities BNL, CERN, DESY, Fermilab, JLab and SLAC;
- Accessed experimentally in deep-inelastic scattering (DIS), semi-inclusive DIS, Drell-Yan, and proton-proton scattering processes;
- Strange PDFs resulting from phenomenological analysis show large uncertainties;

Methodology:

- Results from lattice QCD simulations on the $x-$dependence of PDFs are very promising;
- We presented the first calculation of the flavor decomposition of the helicity PDFs;

  [C. Alexandrou et al., Phys.Rev.Lett. 126 (2021) 10, 102003]

Table of contents

Quasi-PDF approach 1/2

[X. Ji, Phys. Rev. Lett. 110 (2013) 262002 [arXiv:1305.1539]]

- The quasi-PDFs are defined in momentum space

$$\widetilde{q}(x, \mu, P) = 2P_3 \int_{-\infty}^{+\infty} \frac{dz}{4\pi} e^{-ixP_3 z} \mathcal{M}^R(z, P_3),$$

Quasi-PDF approach 1/2

[X. Ji, Phys. Rev. Lett. 110 (2013) 262002 [arXiv:1305.1539]]

- The quasi-PDFs are defined in momentum space

$$\widetilde{q}(x,\mu,P) = 2P_3 \int_{-\infty}^{+\infty} \frac{dz}{4\pi}\, e^{-ixP_3 z}\, \mathcal{M}^R(z,P_3)\,,$$

- Fourier transform of hadronic matrix elements

$$\mathcal{M}^R(z,P_3,\mu) \equiv Z(z,\mu)\,\mathcal{M}(z,P_3)\,,$$

$$\mathcal{M}(z,P_3) \equiv \langle N(P)|\overline{\psi}(z)\,\Gamma\{\mathbf{1},\tau^3\}W(0,z)\psi(0)\,|N(P)\rangle,\ \psi = \begin{pmatrix} u \\ d \end{pmatrix} \text{ or } \psi = s$$

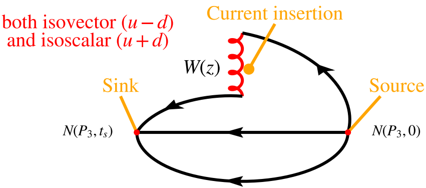

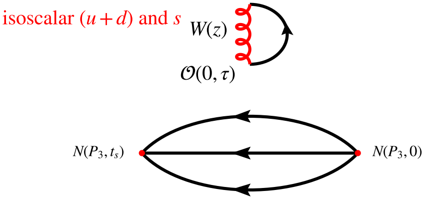

Quasi-PDF approach 1/2

[X. Ji, Phys. Rev. Lett. 110 (2013) 262002 [arXiv:1305.1539]

- The quasi-PDFs are defined in momentum space

$$\widetilde{q}(x, \mu, P) = 2P_3 \int_{-\infty}^{+\infty} \frac{dz}{4\pi} e^{-ixP_3 z} \mathcal{M}^R(z, P_3),$$

- Fourier transform of hadronic matrix elements

$$\mathcal{M}^R(z, P_3, \mu) \equiv Z(z, \mu) \mathcal{M}(z, P_3),$$

$$\mathcal{M}(z, P_3) \equiv \langle N(P)|\overline{\psi}(z) \Gamma\{\mathbf{1}, \tau^3\} W(0, z)\psi(0)|N(P)\rangle, \ \psi = \begin{pmatrix} u \\ d \end{pmatrix} \text{ or } \psi = s$$

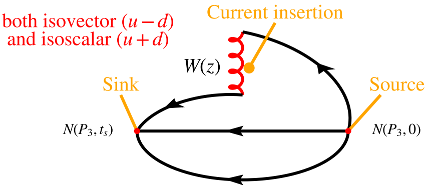

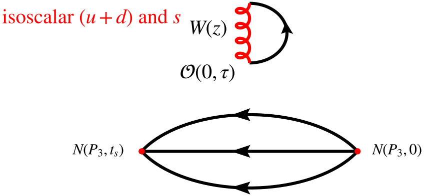

Disconnected contributions much more difficult and expensive to compute!

require the use of appropriate stochastic and gauge-noise reduction techniques

Quasi-PDF approach 2/2

- Evaluation of the renormalization functions $Z(z,\mu)$ in the intermediate $\mathrm{RI}-\mathrm{MOM}$ scheme at μ_0 and conversion to $\mathrm{M}\overline{\mathrm{MS}}$ at μ

  [C. Alexandrou Phys. Rev.D99, 114504 (2019), 1902.00587]

- Quasi-PDFs differ from light-cone PDFs by $\mathcal{O}\left(\Lambda^2_{\mathrm{QCD}}/P_3^2, m_N^2/P_3^2\right)$. This difference can be evaluated in continuum perturbation theory within Large Momentum Effective Theory (LaMET)

$$q(x,\mu) = \int_{-\infty}^{\infty} \frac{d\xi}{|\xi|}\, C\left(\xi, \frac{\mu}{xP_3}\right) \widetilde{q}\left(\frac{x}{\xi}, \mu, P_3\right)$$

  - we employ the one loop matching procedure for the non-singlet case

Quasi-PDF approach 2/2

- Evaluation of the renormalization functions $Z(z, \mu)$ in the intermediate $\mathrm{RI-MOM}$ scheme at μ_0 and conversion to $\mathrm{M\overline{MS}}$ at μ

  [C. Alexandrou Phys. Rev.D99, 114504 (2019), 1902.00587]

- Quasi-PDFs differ from light-cone PDFs by $\mathcal{O}\left(\Lambda^2_{\mathrm{QCD}}/P_3^2, m_N^2/P_3^2\right)$. This difference can be evaluated in continuum perturbation theory within Large Momentum Effective Theory (LaMET)

$$q(x,\mu) = \int_{-\infty}^{\infty} \frac{d\xi}{|\xi|}\, C\left(\xi, \frac{\mu}{xP_3}\right) \widetilde{q}\left(\frac{x}{\xi}, \mu, P_3\right)$$

  - we employ the one loop matching procedure for the non-singlet case

Quasi-PDF approach 2/2

- Evaluation of the renormalization functions $Z(z,\mu)$ in the intermediate $\mathrm{RI}-\mathrm{MOM}$ scheme at μ_0 and conversion to $\mathrm{M}\overline{\mathrm{MS}}$ at μ

  [C. Alexandrou Phys. Rev.D99, 114504 (2019), 1902.00587]

- Quasi-PDFs differ from light-cone PDFs by $\mathcal{O}\left(\Lambda^2_{\mathrm{QCD}}/P_3^2, m_N^2/P_3^2\right)$. This difference can be evaluated in continuum perturbation theory within Large Momentum Effective Theory (LaMET)

$$q(x,\mu) = \int_{-\infty}^{\infty} \frac{d\xi}{|\xi|} C\left(\xi, \frac{\mu}{xP_3}\right) \widetilde{q}\left(\frac{x}{\xi}, \mu, P_3\right)$$

  - we employ the one loop matching procedure for the non-singlet case

- Last step consists of applying the Nucleon Mass Corrections (NMCs) to correct for $m_N/P_3 \neq 0$ in a finite momentum frame

  [J.W. Chen et al., Nucl.Phys. B911 (2016) 246-273,arXiv:1603.06664 [hep-ph]]

Table of contents

Computation of disconnected diagrams

The disconnected quark loop with Wilson line reads

$$\mathcal{L}(t_{\rm ins}, z) = \sum_{\vec{x}_{\rm ins}} \mathrm{Tr}\left[D_q^{-1}(x_{\rm ins}; x_{\rm ins}+z)\Gamma W(x_{\rm ins}, x_{\rm ins}+z)\right]$$

Algorithm

- we computed first $N_{ev} = 200$ eigen-pairs of the squared Dirac twisted-mass operator
- stochastic evaluation of the high-modes contribution to the all-to-all propagator
  - to reduce the contamination of the off diagonal terms up to a coloring distance 2^k ($k = 3$) we employ the hierarchical probing algorithm;
    [A. Stathopoulos et al., 1302.4018]
  - in addition, we make use of the one-end trick;
    [UKQCD, M. Foster and C. Michael, Phys. Rev.D59,074503 (1999), hep-lat/9810021]
    [UKQCD, C. McNeile and C. Michael, Phys. Lett.B556,177 (2003), hep-lat/0212020]
  - fully dilute spin and color subspaces.

We have employed such methods in many recent studies:
[C. Alexandrou et al., (2019), 1909.00485]
[C. Alexandrou et al., (2020), 2003.08486]
[C. Alexandrou et al., (2019) 1909.10744]

[C. Alexandrou et al., Phys. Rev.D100, 014509(2019), 1812.10311]

Numerical setup and statistics

Gauge ensemble with $N_f = 2 + 1 + 1$ twisted mass fermions produced by the Extended Twisted Mass Collaboration

[C. Alexandrou et al., Phys. Rev.D98, 054518 (2018),1807.00495]

$32^3 \times 64$	a=0.0938(3)(2) fm	$m_N = 1.050(8)$ GeV
$L = 3.0$ fm	$m_\pi \approx 260$ MeV	$m_\pi L \approx 4.0$

Numerical setup and statistics

Gauge ensemble with $N_f = 2 + 1 + 1$ twisted mass fermions produced by the Extended Twisted Mass Collaboration

[C. Alexandrou et al., Phys. Rev.D98, 054518 (2018),1807.00495]

$32^3 \times 64$	a=0.0938(3)(2) fm	$m_N = 1.050(8)$ GeV
$L = 3.0$ fm	$m_\pi \approx 260$ MeV	$m_\pi L \approx 4.0$

Statistics disconnected diagrams

	Loops					Two-point functions		
P_3 [GeV]	$N_{\rm ev}$	$N_{\rm conf}$	$N_{\rm had}$	$N_{\rm sc}$	$N_{\rm inv}$	$N_{\rm srcs}$	$N_{\rm dir}$	$N_{\rm meas}$
0.41	200	330	512	12	6144	200	6	$396 \cdot 10^3$
0.83	200	349	512	12	6144	200	6	$418.8 \cdot 10^3$
1.24	200	1103	512	12	6144	200	6	$1.3236 \cdot 10^6$
1.65	200	1160	512	12	6144	200	6	$1.392 \cdot 10^6$

Numerical setup and statistics

Gauge ensemble with $N_f = 2 + 1 + 1$ twisted mass fermions produced by the Extended Twisted Mass Collaboration

[C. Alexandrou et al., Phys. Rev.D98, 054518 (2018),1807.00495]

$32^3 \times 64$	a=0.0938(3)(2) fm	$m_N = 1.050(8)$ GeV
$L = 3.0$ fm	$m_\pi \approx 260$ MeV	$m_\pi L \approx 4.0$

Statistics disconnected diagrams

	Loops					Two-point functions		
P_3 [GeV]	$N_{\rm ev}$	$N_{\rm conf}$	$N_{\rm had}$	$N_{\rm sc}$	$N_{\rm inv}$	$N_{\rm srcs}$	$N_{\rm dir}$	$N_{\rm meas}$
0.41	200	330	512	12	6144	200	6	$396 \cdot 10^3$
0.83	200	349	512	12	6144	200	6	$418.8 \cdot 10^3$
1.24	200	1103	512	12	6144	200	6	$1.3236 \cdot 10^6$
1.65	200	1160	512	12	6144	200	6	$1.392 \cdot 10^6$

Statistics connected diagrams

P_3 [GeV]	$N_{\rm conf}$	$N_{\rm src}$	$N_{\rm meas}$	t_s [fm]
0.41	50	8	400	0.94
0.83	194	8	1552	1.13
1.24	709	14	9926	1.13

Table of contents

Strange matrix elements

Momentum dependence

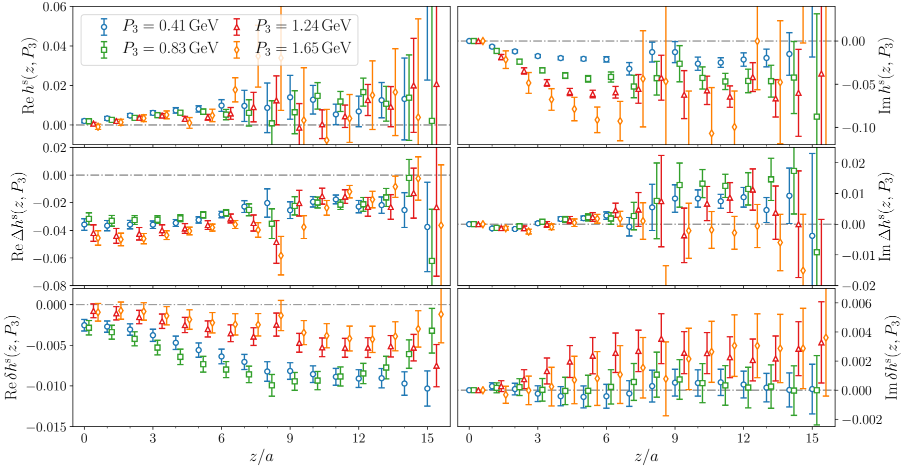

Disconnected isoscalar matrix elements

Momentum dependence

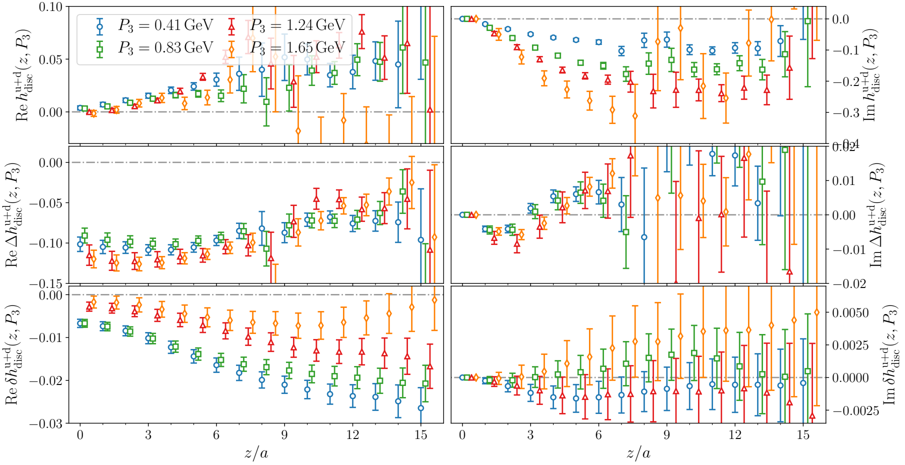

Light quark distributions

Comparison with phenomenology

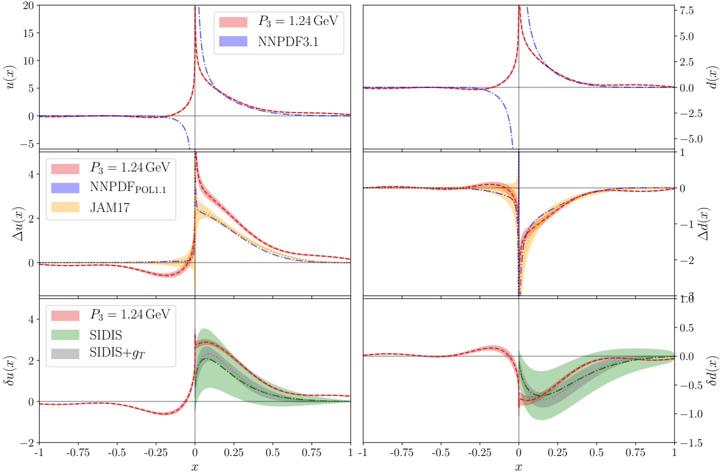

NNPDF
[Nucl. Phys. B887, 276 (2014)]
[Eur. Phys. J. C77, 663 (2017)]

JAM
[Phys. Rev. Lett. 119, 132001 (2017)]
[Phys. Rev. Lett.120, 152502 (2018)]

Strange quark distributions

Comparison with phenomenology

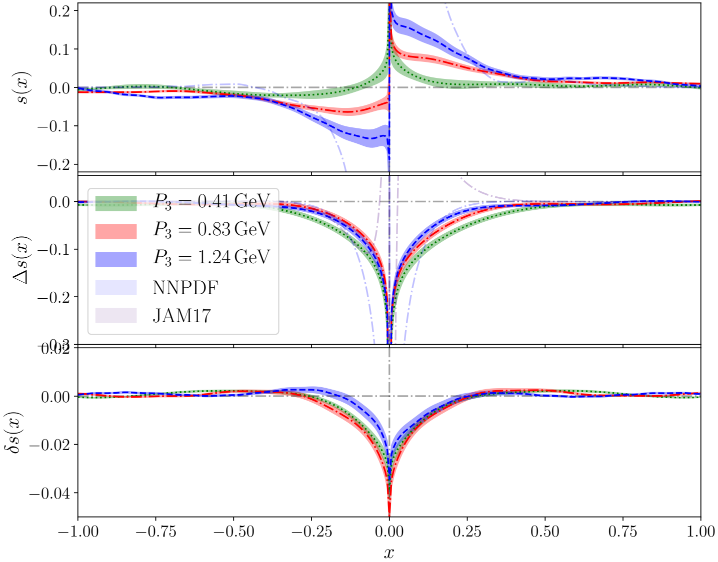

Systematic effects

Different systematic effects still need to be adressed:

1. pion mass [Alexandrou et al., Phys. Rev. Lett.121,112001 (2018), 1803.02685]

Systematic effects

Different systematic effects still need to be adressed:

1. pion mass [Alexandrou et al., Phys. Rev. Lett.121,112001 (2018), 1803.02685]
2. finite P_3 and t_s
   - the signal exponentially deteriorates with P_3 and with t_s;
   - to take into account the excited stated effect $t_s \gtrsim 1\,\mathrm{fm} \Rightarrow$ at high P_3 this becomes very challenging;
   - momentum smearing effectively helps reducing the signal-to-noise ratio, but the noise still scales exponentially with P_3;

Systematic effects

Different systematic effects still need to be adressed:

1. pion mass [Alexandrou et al., Phys. Rev. Lett.121,112001 (2018), 1803.02685]
2. finite P_3 and t_s
   - the signal exponentially deteriorates with P_3 and with t_s;
   - to take into account the excited stated effect $t_s \gtrsim 1\,\mathrm{fm}$ $\Rightarrow$ at high P_3 this becomes very challenging;
   - momentum smearing effectively helps reducing the signal-to-noise ratio, but the noise still scales exponentially with P_3;
3. cut-off effects

Systematic effects

Different systematic effects still need to be adressed:

1. pion mass [Alexandrou et al., Phys. Rev. Lett.121,112001 (2018), 1803.02685]
2. finite P_3 and t_s
   - the signal exponentially deteriorates with P_3 and with t_s;
   - to take into account the excited stated effect $t_s \gtrsim 1\,\mathrm{fm} \;\Rightarrow$ at high P_3 this becomes very challenging;
   - momentum smearing effectively helps reducing the signal-to-noise ratio, but the noise still scales exponentially with P_3;
3. cut-off effects
4. truncation of conversion between renormalization schemes and matching
   Two-loops matching [L.-B. Chen et al., 2020, 2005.13757, 2006.10917, 2006.14825]

Systematic effects

Different systematic effects still need to be adressed:

1. pion mass [Alexandrou et al., Phys. Rev. Lett.121,112001 (2018), 1803.02685]
2. finite P_3 and t_s
   - the signal exponentially deteriorates with P_3 and with t_s;
   - to take into account the excited stated effect $t_s \gtrsim 1\,\mathrm{fm} \Rightarrow$ at high P_3 this becomes very challenging;
   - momentum smearing effectively helps reducing the signal-to-noise ratio, but the noise still scales exponentially with P_3;
3. cut-off effects
4. truncation of conversion between renormalization schemes and matching
   Two-loops matching [L.-B. Chen et al., 2020, 2005.13757, 2006.10917, 2006.14825]
5. singlet renormalization and matching

Systematic effects

Different systematic effects still need to be adressed:

1. pion mass [Alexandrou et al., Phys. Rev. Lett.121,112001 (2018), 1803.02685]
2. finite P_3 and t_s
   - the signal exponentially deteriorates with P_3 and with t_s;
   - to take into account the excited stated effect $t_s \gtrsim 1\,\mathrm{fm} \Rightarrow$ at high P_3 this becomes very challenging;
   - momentum smearing effectively helps reducing the signal-to-noise ratio, but the noise still scales exponentially with P_3;
3. cut-off effects
4. truncation of conversion between renormalization schemes and matching
   Two-loops matching [L.-B. Chen et al., 2020, 2005.13757, 2006.10917, 2006.14825]
5. singlet renormalization and matching

To be addressed in the future!

Table of contents

Conclusions

Results obtained so far:

- ☑ First computation of the disconnected contributions to the isoscalar unpolarized, helicity and transversity matrix elements at $m_\pi \approx 260\,\mathrm{MeV}$;

Conclusions

Results obtained so far:

- ☑ First computation of the disconnected contributions to the isoscalar unpolarized, helicity and transversity matrix elements at $m_\pi \approx 260\,\mathrm{MeV}$;
- ☑ Renormalization and matching of the isoscalar and isovector matrix elements, allowing to compute the light quarks distributions;

Conclusions

Results obtained so far:

- ☑ First computation of the disconnected contributions to the isoscalar unpolarized, helicity and transversity matrix elements at $m_\pi \approx 260\,\mathrm{MeV}$;
- ☑ Renormalization and matching of the isoscalar and isovector matrix elements, allowing to compute the light quarks distributions;
- ☑ Computation of the strange quark unpolarized, helicity and transversity distributions;

Conclusions

Results obtained so far:

- ☑ First computation of the disconnected contributions to the isoscalar unpolarized, helicity and transversity matrix elements at $m_\pi \approx 260\,\mathrm{MeV}$;
- ☑ Renormalization and matching of the isoscalar and isovector matrix elements, allowing to compute the light quarks distributions;
- ☑ Computation of the strange quark unpolarized, helicity and transversity distributions;

the comparison with phenomenological data looks very promising!

Conclusions

Results obtained so far:

- ☑ First computation of the disconnected contributions to the isoscalar unpolarized, helicity and transversity matrix elements at $m_\pi \approx 260\,\mathrm{MeV}$;
- ☑ Renormalization and matching of the isoscalar and isovector matrix elements, allowing to compute the light quarks distributions;
- ☑ Computation of the strange quark unpolarized, helicity and transversity distributions;

the comparison with phenomenological data looks very promising!

Future steps:

- ☐ In depth evaluation of the systematic effects;

Conclusions

Results obtained so far:

- ☑ First computation of the disconnected contributions to the isoscalar unpolarized, helicity and transversity matrix elements at $m_\pi \approx 260\,\mathrm{MeV}$;
- ☑ Renormalization and matching of the isoscalar and isovector matrix elements, allowing to compute the light quarks distributions;
- ☑ Computation of the strange quark unpolarized, helicity and transversity distributions;

the comparison with phenomenological data looks very promising!

Future steps:

- ☐ In depth evaluation of the systematic effects;
- ☐ Exploratory study of the distributions at the physical point;

Conclusions

Results obtained so far:

- ☑ First computation of the disconnected contributions to the isoscalar unpolarized, helicity and transversity matrix elements at $m_\pi \approx 260\,\mathrm{MeV}$;
- ☑ Renormalization and matching of the isoscalar and isovector matrix elements, allowing to compute the light quarks distributions;
- ☑ Computation of the strange quark unpolarized, helicity and transversity distributions;

the comparison with phenomenological data looks very promising!

Future steps:

- ☐ In depth evaluation of the systematic effects;
- ☐ Exploratory study of the distributions at the physical point;

Thank you for your attention!

This project has received funding from the European Union's Horizon 2020 research and innovation programme under grant agreement No 765048.